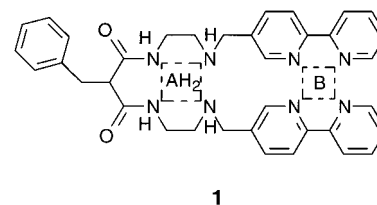


Signal Amplification by a Fluorescent Indicator of a pH-Driven Intramolecular Translocation of a Copper(II) Ion**

Valeria Amendola, Luigi Fabbrizzi,* Carlo Mangano, Hamish Miller, Piersandro Pallavicini, Angelo Perotti, and Angelo Taglietti



The translocation of a metal ion in a reversible and repeatable manner from one compartment to the other within a ditopic ligand could lead to mechanical work at the molecular level.^[1] This possibility gives rise to a new class of potential artificial molecular machines,^[2] thus adding to the possibilities based on rotaxanes and catenanes.^[3,4] Movement of metal ions, which takes place following a predetermined pathway, can be induced by different stimuli, such as a variation of the redox potential,^[5,6] or a pH change.^[7] The use of pH as the stimulus is especially convenient as it involves a rather mild perturbation and does not cause degradation of the system, and hence its operation can be repeated at will, indefinitely. This situation is not always the case with the more drastic and destructive processes which involve an auxiliary oxidation and reduction reaction. The essential requirements for the occurrence of a pH-driven metal translocation process are that 1) one of the two coordinating compartments (A) also shows a distinct acid–base behavior (for example, through the $AH_n \rightleftharpoons A^{n-} + nH^+$ equilibrium), and that 2) the coordinating tendencies of the two compartments decrease along the series $A^{n-} \gg B \gg AH_n$, where B is the second compartment that does not display acid–base behavior, at least in the investigated pH interval. Thus, at a pH value in which AH_n dominates, the metal ion stays in compartment B. On the other hand, when the pH value is increased and AH_n deprotonates, the metal ion moves to the more appealing compartment A^{n-} . The metal ion moves back to B on decreasing the pH value. In the case of transition metal ions, a change in the compartment typically modifies the stereochemistry and the ligand field experienced by the cation, thus altering its electronic structure and spectral features. Ultimately, the displacement of the metal ion is signaled by a color change of the solution. We show here that the position of the metal ion in the ditopic system can be determined by the powerful signal of a fluorescent indicator (which is present at a very low concentration) provided that the indicator is able to interact selectively with the metal ion.

The envisaged ditopic ligand **1** contains two distinct tetradentate compartments: A and B. The donor set of A consists of two secondary amine and two secondary amide nitrogen atoms. As the amide group itself possesses poor or no

coordinating tendencies, the neutral form AH_2 is expected to display minimum binding tendencies towards the chosen metal ion, Cu^{II} . On the other hand, at neutral or slightly alkaline pH values, the amide group deprotonates in the presence of divalent late-transition-metal ions to give rise to a very strong donor group: thus, the doubly deprotonated A^{2-} compartment is expected to establish especially intense metal–ligand interactions and give rise to a very stable complex with a square geometry. Compartment B is constituted by two 2,2'-bipyridine (bpy) fragments, which display fairly good binding tendencies towards Cu^{II} ions. Complexes of the $[Cu^{II}(bpy)_2]^{2+}$ type tend to be five coordinate, the remaining coordination site being occupied by a solvent molecule or by a coordinating anion. Thus, it appears that the required sequence of affinity ($A^{2-} \gg B \gg AH_2$) is established and that the Cu^{II} ion can be translocated between B and A and vice versa over a defined pH range.

We used a dioxane/water mixture (4:1) as the solvent. Pure water could not be used because of the precipitation of Cu^{II} complexes in alkaline conditions. We carried out potentiometric titration experiments and, through nonlinear least-squares treatment of titration data,^[8] we calculated the formation constants of the species present in equilibrium between pH 2 and 12. We were then able to draw the corresponding distribution curves (Figure 1).

Two major metal-containing species are present in alkaline conditions in a solution containing equimolar amounts of **1** (LH_2) and Cu^{II} ions. A species $[Cu^{II}(LH_2)]^{2+}$ reaches its maximum abundance (80 %) at pH 7.4, and a species $[Cu^{II}(L)]$ reaches 100 % abundance at $pH \geq 11$.

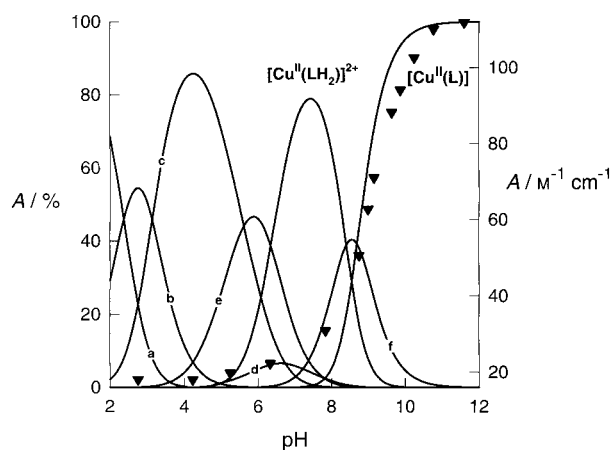


Figure 1. Concentration of the species present at the equilibrium in a solution containing equimolar amounts of **1** ($=LH_2$) and Cu^{2+} ions; profiles **a**, **b**, **c**, and **d** refer to the variously protonated forms of LH_2 (from LH_6^{4+} to LH_3^+). Profile **e** refers to the metal-containing protonated species $[Cu^{II}(LH_3)]^{3+}$. Profile **f** refers to the metal-containing species $[Cu^{II}(LH_2)(OH)]^+$. Full triangles give the molar absorptance of the d–d band ($\lambda_{max} = 502$ nm) of the $[Cu^{II}(L)]$ complex.

[*] Prof. L. Fabbrizzi, Dr. V. Amendola, Dr. C. Mangano, Dr. H. Miller, Dr. P. Pallavicini, Prof. A. Perotti, Dr. A. Taglietti
Dipartimento di Chimica Generale
Università di Pavia
via Taramelli 12, 27100 Pavia (Italy)
Fax: (+39)0382-528-544
E-mail: luigi.fabbrizzi@unipv.it

[**] This work was supported by the European Union (RT Network Molecular Level Devices and Machines: Contract HPRN-CT-2000-00029) and by the Italian Ministry of University and Research (PRIN—Progetto “Dispositivi Supramolecolari”).

Noticeably, the absorption spectrum of the blue solution at pH 7.4 (Figure 2) is very similar to that of a solution of the $[\text{Cu}^{\text{II}}(\text{bpy})_2]^{2+}$ model complex. This observation indicates that the metal ion stays in compartment B. Moreover, the mass spectra (ESI) recorded at this pH value display peaks at m/z 776, 778, and 780 which correspond to $[\text{Cu}^{\text{II}}(\text{LH}_2)]^+$, $[\text{Cu}^{\text{II}}(\text{LH}_2)]^+$, and $[\text{Cu}^{\text{II}}(\text{LH}_2)]^+$, as expected.

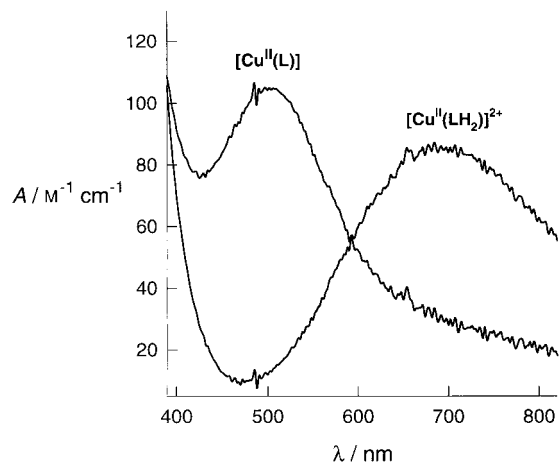


Figure 2. d-d spectra of the $[\text{Cu}^{\text{II}}(\text{LH}_2)]^{2+}$ complex (blue, Cu^{2+} stays in compartment B) and of the $[\text{Cu}^{\text{II}}(\text{L})]^{2+}$ complex (pink/violet, Cu^{2+} stays in compartment A).

On the other hand, adjusting the pH value to 12 by the addition of standard base makes the solution become pink/violet. The color and the absorption spectrum are similar to that observed for the model complex with a tetradentate ligand containing two deprotonated amide groups and two amine groups ($\text{NH}_2\text{CH}_2\text{CH}_2\text{NH}(\text{CO})\text{CH}_2\text{CH}_2\text{CH}_2\text{NH}(\text{CO})\text{CH}_2\text{CH}_2\text{NH}_2$ (dioxo-2,3,2-tet)). This evidence suggests that the metal ion in the species dominating at $\text{pH} \geq 11$ ($[\text{Cu}^{\text{II}}(\text{L})]$) is located in compartment A^{2-} (Figure 2). Further evidence is derived from pH-dependent spectrophotometric measurements. In particular, the intensity of the band at 502 nm superimposes well on the abundance profile of the $[\text{Cu}^{\text{II}}(\text{L})]$ species. Moreover, the ESI mass spectrum recorded at pH 12 displays the signal of the expected species, $[\text{Cu}^{\text{II}}(\text{L}) + \text{Na}]^+$, with m/z 698, 700 (Na^+ comes from the added standard base). The solution turns blue again on addition of standard acid back to pH 7.4, which indicates that the reverse translocation has taken place. The direct and reverse translocation processes can be repeated at will, in principle indefinitely. The detection limit is determined by the progressive dilution of the solution, which arises as a result of the consecutive addition of the standard solutions of acid and base.

The rate of the metal ion translocation, both direct and reverse, could be determined by stopped-flow spectrophotometric experiments. In particular, the B-to-A metal ion displacement could be monitored through the development of the absorption band at 502 nm, which corresponds to the formation of the pink/violet $[\text{Cu}^{\text{II}}(\text{L})]$ species. The absorbance versus time profile strictly fits a first-order kinetics, with a lifetime τ of 0.54 ± 0.05 s. The first-order A-to-B translocation,

investigated through the decay of the band at 502 nm, exhibits a lifetime τ of 0.58 ± 0.05 s. First-order patterns observed for both direct and reverse processes indicate the intramolecular nature of the translocation. No details are available on the intimate mechanism of the processes. It is probable that the minor species which forms at pH 8.5 plays some role. The formula $[\text{Cu}^{\text{II}}(\text{L})\text{OH}]^+$ is assigned to this singly charged species: the hydroxide ion results from the deprotonation of the water molecule bound to the Cu^{II} ion in the five-coordinate complex in compartment B.

The reversible translocation can be followed through a more powerful signal, fluorescence, by making use of an auxiliary light-emitting fragment, namely coumarin-343 (FIH, **2**). This molecule is a protic acid, since it contains a carboxylic acid group, whose pK_A value in the 4:1 dioxane/water solution is 7.30 ± 0.02 . The undissociated form FIH is strongly fluorescent, with an emission band centered at $\lambda_{\text{max}} = 490$ nm; the emission band of the dissociated form (FI^-) is less intense (fluorescence intensity (I_F) is 75 % that of FIH) and is blue-shifted to 471 nm (λ_{max}). Thus, a solution of coumarin-343 (for example, 2×10^{-6} M) is fluorescent over the entire pH range, even if a change in the I_F and λ_{max} values is observed in the pH 6.5–8.5 range. If the same solution is also made 4×10^{-4} M in the copper(II) complex of **1** (a concentration 220 times higher than that of FIH), the pH dependence of the fluorescence intensity corresponding to the FIH and FI^- bands changes drastically.

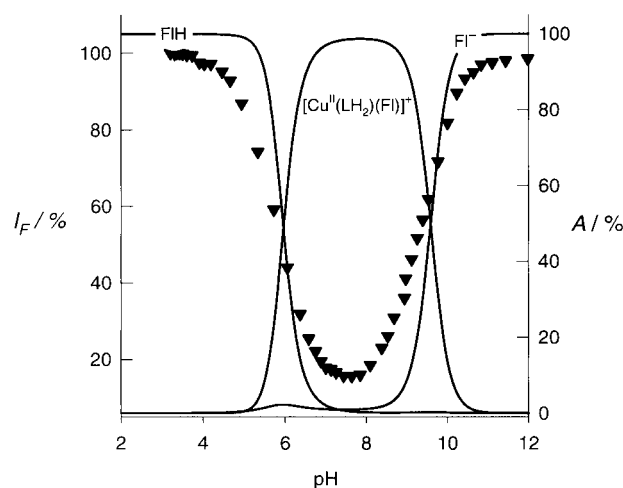
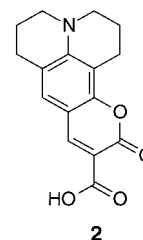


Figure 3. Full triangles (left vertical axis) indicate the fluorescence intensity (I_F) of a solution containing 2×10^{-6} M coumarin-343 (**2**) and 4×10^{-4} M of the $[\text{Cu}^{\text{II}}(\text{LH}_2)]^{2+}/[\text{Cu}^{\text{II}}(\text{L})]$ complex: values of the descending arm of the well-shaped profile refer to the emission band at 490 nm (emitting fragment: coumarin-343, undissociated form, FIH); values of the ascending arm refer to the emission band at 471 nm (emitting fragment: dissociated form, FI^-). I_F values are normalized. Solid lines (right vertical axis) give the pH dependance of the concentration of FIH, $[\text{Cu}^{\text{II}}(\text{LH}_2)(\text{FI})]^+$, and FI^- in the same solution. Moving up from pH 7, by the absence of fluorescence (bottom of the well) signals that the Cu^{II} ion stays in compartment B, while the presence of fluorescence signals that the Cu^{II} ion is in compartment A.

pH 7–8, then it increases again (according to a well-shaped profile) to reach a plateau at pH > 11.5. This behavior can be accounted for by assuming that in the pH interval where the well of the I_F plot is present, the $[\text{Cu}^{\text{II}}(\text{LH}_2)(\text{H}_2\text{O})]^{2+}$ species forms and the carboxylate group of FI^- replaces the water molecule coordinated to the Cu^{II} center in the B compartment. The binding of FI^- to the transition metal ion causes a quenching of the fluorescence, through either an electron-transfer or an energy-transfer process. At pH > 11.5, when more than 99.8% of the metal has translocated to the A^{2-} site, a planar complex is formed, which, as a result of the very strong in-plane interaction, does not exhibit any affinity towards further ligands. As a consequence, FI^- is released to the solution and displays its full fluorescence. Thus, B-to-A translocation is signaled by the switching-on of the fluorescence. On the other hand, A-to-B translocation, induced by adjusting the pH value back to 7–8, is signaled by the switching-off of the fluorescence. One can switch the pH values back and forth many times and, as a result of the high efficiency of the fluorescence signal, the occurrence of the reversible translocation can be perceived each time, both visually and instrumentally.

A binding constant of 5.5 ± 0.1 log units was found from the spectrofluorimetric data for the equilibrium: $[\text{Cu}^{\text{II}}(\text{LH}_2)(\text{H}_2\text{O})]^{2+} + \text{FI}^- \rightleftharpoons [\text{Cu}^{\text{II}}(\text{LH}_2)(\text{FI})]^+ + \text{H}_2\text{O}$. Thus, it was possible to draw the distribution diagram shown in Figure 3. This plot indicates that the $[\text{Cu}^{\text{II}}(\text{LH}_2)(\text{FI})]^+$ adduct begins to form at pH 4.5, which causes fluorescence quenching (left arm of the well, \blacktriangledown). On the other hand, a decrease in the $[\text{Cu}^{\text{II}}(\text{LH}_2)(\text{FI})]^+$ concentration, which is associated with a translocation to A, corresponds to the release of the FI^- light-emitting species and to the generation of fluorescence (right arm of the well, \blacktriangledown).

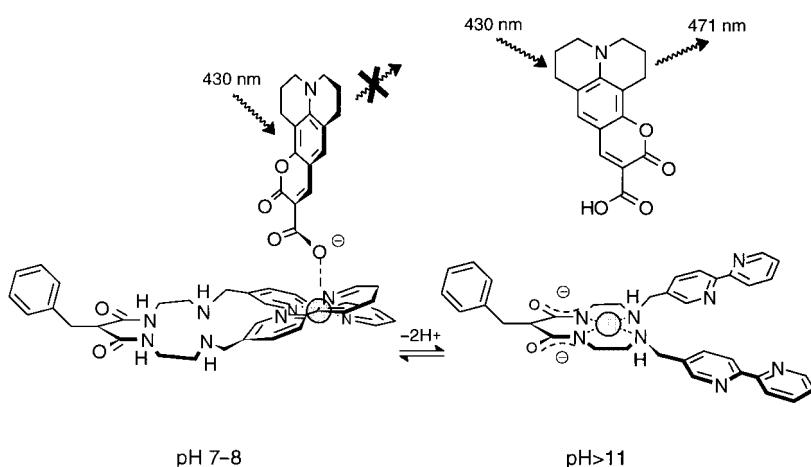
Scheme 1 provides a pictorial sketch of the hypothesized stereochemical aspects of metal translocation and of complexation/decomplexation of FI^- . It has to be noted that metal displacement in a previously described pH-driven Cu^{II} translocation experiment involved drastic rearrangement and folding of the ligating framework.^[9] In the present case, each compartment displays a distinct coordinating behavior and does not interfere with metal binding by the other compartment.

Translocation of a transition metal ion between the unequivalent compartments of a ditopic ligand is an interesting switching process, which can be read by monitoring a variety of properties (spectroscopic, magnetic, electrochemical). Among these properties, fluorescence is undoubtedly one of the most advantageous, as it is visual and can be detected instrumentally with extreme sensitivity. A rational, but very time consuming, way to profit from fluorescence involves the synthesis of ligands, to whose framework a given fluorophore has been covalently bound. However, this approach can be highly perturbative, as the sterically hindering fluorogenic substituent may strongly reduce the rate of metal-ion movement. In a reported example,^[7] the covalent linking of a fluorescent fragment (anthracene) to the framework of the ditopic ligand made the translocation rate of the metal ion (Ni^{II}) decrease by an order of magnitude with respect to a system without steric hinderance (the τ value varied from hundreds of milliseconds to seconds). On the other hand, the use of an auxiliary fluorescent indicator that possesses coordinating tendencies is not perturbative at all, particularly because it is present at an extremely low concentration (220 times lower than that of the $[\text{Cu}^{\text{II}}(\text{LH}_2)]^{2+}$ complex). Moreover, in spite of the fact that FI^- binds only a small fraction of $[\text{Cu}^{\text{II}}(\text{LH}_2)]^{2+}$ ions, a powerful ON/OFF signal is detected even after many cycles and remarkable dilution. The only prerequisite the designer should address is that of the two compartments: one should provide coordinative unsaturation and the other should not. Fluorescent indicators recently experienced a revival in the sensing of recognition events.^[10] In particular, coumarin-343 has been used as an OFF/ON indicator to signal the recognition of HCO_3^- ions by a dicopper(II) bis-tren cryptate (tren = tris(2-ethylamino)-amine).^[11] It appears now that fluorescent indicators can also be profitably utilized to signal the movements occurring at the molecular level and to monitor the working of molecular machines.

Experimental Section

Ligand **1** was synthesized through the Schiff-base reaction of 6-benzyl-1,4,8,11-tetraazaundecane-5,8-dione^[7] (1 mmol) with 5-(2,2')-bipyridine-carboxyaldehyde^[12] (2 mmol) in ethanol (20 mL, room temperature, 24 h), followed by in situ reduction with an excess of NaBH_4 (0.8 g). The solvent was removed from the reaction mixture on a rotary evaporator and the solid residue was treated with 0.1M NaOH (20 mL). Extraction with CH_2Cl_2 , drying with MgSO_4 , and removal of the solvent under vacuum gave the desired product as a solid in 35% yield. Elemental analysis calcd (%) for $\text{C}_{36}\text{H}_{38}\text{N}_8\text{O}_2$: C 70.37, H 6.18, N 18.23; found C 70.41, H 6.16, N 18.20. MS (ESI): m/z : 615 [**1** + H^+]; ^1H NMR (CDCl_3): δ = 8.72 (d, 2H, Ar-H), 8.60 (s, 2H, Ar-H), 8.48 (t, 2H, Ar-H), 7.78 (m, 4H, Ar-H), 7.1–7.3 (m, 9H, Ar-H), 6.95 (brt, 2H, CONH), 3.79 (s, 4H, NHCH_2 -bipyridine), 3.38–3.20 (m, 7H, $\text{CONHCH}_2\text{CH}_2 + \text{PhCH}_2\text{CH}$), 2.65 (m, 4H, CONHCH_2), 2.15 (br, CH_2NHCH_2).

Received: December 27, 2001
Revised: April 22, 2002 [Z18443]



Scheme 1.

- [1] J.-M. Lehn, *Supramolecular Chemistry, Concepts and Perspectives*, VCH, Weinheim, 1995, pp. 124–127.
- [2] V. Amendola, L. Fabbri, C. Mangano, P. Pallavicini, *Acc. Chem. Res.* **2001**, 34, 488–493.

- [3] V. Balzani, A. Credi, F. M. Raymo, J. F. Stoddart, *Angew. Chem.* **2000**, *112*, 3484–3530; *Angew. Chem. Int. Ed.* **2000**, *39*, 3348–3391.
 [4] J.-P. Sauvage, *Acc. Chem. Res.* **1998**, *31*, 611–619.
 [5] L. Zelikovitch, J. Libman, A. Shanzler, *Nature* **1995**, *374*, 790–792.
 [6] T. R. Ward, A. Lutz, S. P. Parel, J. Ensling, P. Güttlich, P. Buglyó, C. Orvig, *Inorg. Chem.* **1999**, *38*, 5007–5017.
 [7] V. Amendola, L. Fabbri, C. Mangano, P. Pallavicini, A. Perotti, A. Taglietti, *J. Chem. Soc. Dalton Trans.* **2000**, 185–189.
 [8] P. Gans, A. Sabatini, A. Vacca, *Talanta* **1996**, *43*, 1739–1753.
 [9] V. Amendola, C. Brusoni, L. Fabbri, C. Mangano, H. Miller, P. Pallavicini, A. Perotti, A. Taglietti, *J. Chem. Soc. Dalton Trans.* **2001**, 3528–3533.
 [10] E. V. Anslyn, *Acc. Chem. Res.* **2001**, *34*, 963–972.
 [11] L. Fabbri, A. Leone, A. Taglietti, *Angew. Chem.* **2001**, *113*, 3156–3159; *Angew. Chem. Int. Ed.* **2001**, *40*, 3066–3069.
 [12] V. Balzani, V. Polin, E. Schmohel, *Synthesis* **1998**, *3*, 321–324.

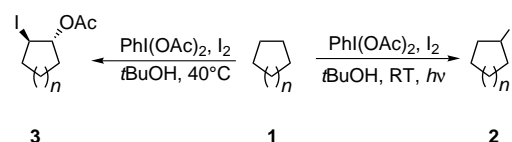
Activation of Alkanes upon Reaction with $\text{PhI}(\text{OAc})_2 - \text{I}_2^{**}$

José Barluenga,* Francisco González-Bobes, and José M. González

Carbon–hydrogen-bond-activation reactions are challenging processes in organic synthesis.^[1] Halogenation reactions have been thoroughly studied and widely practiced and provide a simple and classic way to functionalize hydrocarbons.^[2] However, the iodination of alkanes has been a particularly elusive reaction and still remains as an active research area.^[3] The endothermic nature of the overall process has been invoked to explain the failure of a radical-chain approach to accomplish this reaction.^[4, 5] While performing β -scission reactions of cycloalkanols,^[6] we noticed that (diacetoxyiodo)benzene $[\text{PhI}(\text{OAc})_2]$ ^[7] gave rise to a mixture of compounds, where iodocyclohexane (**2b**) was found as the major product, resulting from an activation of the cyclohexane used as solvent.

Herein we report new approaches to selectively produce either iodoalkanes **2** or 1-acetoxy-2-iodocycloalkanes **3** from readily available hydrocarbons **1**. The products **2** and **3** arise from single and double formal C–H-bond-activation reactions, respectively. This unique reaction manifold can be tuned by treating alkanes **1** with $\text{PhI}(\text{OAc})_2$, iodine (I_2), and *tert*-butylalcohol (*t*BuOH) simply by using photochemical or thermal conditions (Scheme 1).

Our initial studies with cyclohexane (**1b**) showed that the presence of an alcohol is necessary for an efficient alkane activation. *t*BuOH was found to be the most effective of all the alkanols tested. Thus, cycloalkanes were cleanly converted



Scheme 1. Photochemical and thermal reactivity of hydrocarbons with $\text{PhI}(\text{OAc})_2 - \text{I}_2$.

into the corresponding iodinated derivatives, under irradiation conditions (2×100 W lamps), in high yield, under relatively mild conditions, and in rather short reaction times. In addition, toluene (**1e**) also gives benzyl iodide (**2e**) as the sole reaction product.^[8] Linear alkanes react affording mixtures of monoiodinated derivatives in good combined yield, showing high selectivity for secondary positions (Table 1).

An outstanding feature of this iodine(III)-induced activation of alkanes was observed when carrying out the reactions under thermal instead of photochemical conditions.^[9] In this case, bifunctional compounds **3** were obtained as major, or even single, reaction products (Scheme 1, Table 2). The global

Table 1. Synthesis of iodoalkanes **2** from alkanes **1**.^[a]

Entry	Alkane (1)	Concentration [M] ^[b]	Reaction time [h]	Product (2)	Yield [%] ^[c]
1		0.04	1.5		98
2		0.04	4		97
3		0.02	6		92
4		0.02	8		85 ^[d]
5		0.02	1		92 ^[e]
6		0.04	4		85 ^[f]

[a] All reactions performed with the following stoichiometry: $\text{PhI}(\text{OAc})_2$ (1 equiv), I_2 (1.1 equiv), *t*BuOH (1 equiv). The alkane was used as solvent. [b] Referred to iodine. [c] GC yield unless otherwise specified. [d] Compound **2d** was isolated in 80% yield upon column chromatography with *n*-hexane as eluant. [e] Determined by ^1H NMR spectroscopy. [f] Proportions of isomers (determined by GC): **2g**:**2h** = 1:1.5, **2f**:**2g** + **2h** = 1:15.

[*] Prof. Dr. J. Barluenga, F. González-Bobes, Dr. J. M. González
 Instituto de Química Organometálica “Enrique Moles”
 Unidad Asociada al C.S.I.C.
 Universidad de Oviedo
 33071 Oviedo (Spain)
 Fax: (+34) 98-510-3450
 E-mail: barluenga@sauron.quimica.uniovi.es

[**] This research was supported by DGES (Grant PB97-1271). F.G.-B. thanks FICYT for a fellowship.